

Measurement of Side-Chain Carboxyl pK_a Values of Glutamate and Aspartate Residues in an Unfolded Protein by Multinuclear NMR Spectroscopy

Martin Tollinger,[†] Julie D. Forman-Kay,^{†,‡,||} and Lewis E. Kay^{*,‡,§,||}

Contribution from the Structural Biology and Biochemistry Program, Hospital for Sick Children, Toronto, Ontario, Canada M5G 1X8, Department of Biochemistry, University of Toronto, Toronto, Ontario, Canada M5S 1A8, Departments of Medical Genetics and Chemistry, University of Toronto, Toronto, Ontario, Canada M5S 1A8, and Protein Engineering Network Centers of Excellence

Received January 14, 2002. Revised Manuscript Received March 4, 2002

Abstract: A triple-resonance NMR pulse scheme is presented for measuring aspartic and glutamic acid side-chain pK_a values in unfolded protein states where chemical shift overlap is limiting. The experiment correlates side-chain carboxyl carbon chemical shifts of these residues with the backbone amide proton chemical shift of the following residue. The methodology is applied to an ^{15}N , ^{13}C labeled sample of the N-terminal SH3 domain of the *Drosophila* protein drk, which exists in equilibrium between folded (F_{exch}) and unfolded (U_{exch}) states under nondenaturing conditions. Residue-specific pK_a values of side-chain carboxyl groups are presented for the first time for an unfolded protein (drk U_{exch} state), determined from a pH titration. Results indicate that deviations from pK_a values measured for model compounds are likely due to local effects, while long-range electrostatic interactions appear to be of minor importance for this protein.

Introduction

Side-chain carboxyl pK_a values of aspartic and glutamic acid moieties in proteins provide important information on the electrostatic environment of these residues.^{1–3} In folded proteins, residue-specific pK_a values for Asp and Glu carboxylates can be measured by monitoring the pH dependence of side-chain carboxyl carbon ($^{13}\text{C}^\gamma$ in Asp, or $^{13}\text{C}^\delta$ in Glu) chemical shifts or of proton chemical shifts ($^1\text{H}^\beta$ in Asp, $^1\text{H}^\gamma$ in Glu or other nearby protons), using a variety of one²- and two⁴-dimensional NMR approaches. In contrast, in the case of unfolded proteins, ^1H and ^{13}C chemical shifts for Asp and Glu residues are often significantly overlapped, rendering a quantitative analysis using existing methodology extremely difficult or impossible.

Measurement of pK_a values for titratable groups in an unfolded protein is of particular interest since such values can provide insight into whether there are charge–charge interactions in the molecule and whether these might be native or non-

native. Moreover, since the pH dependence of the stability of a protein depends on the difference in charge between folded and unfolded forms, knowledge of pK_a values for the unfolded state is critical for understanding the pH dependence of protein stability.⁵ We present here for the first time site-specific pK_a values for Asp and Glu residues in an unfolded protein state obtained with a new triple-resonance NMR pulse scheme which correlates Asp/Glu side-chain carboxyl ^{13}C chemical shifts with the backbone amide proton $^1\text{H}^\text{N}$ shift of the following residue. The experiment is applied to a uniformly $^{15}\text{N}/^{13}\text{C}$ labeled sample of the N-terminal SH3 domain (59 residues) of the *Drosophila* protein drk (drkN SH3 domain), which exists in equilibrium between folded and unfolded states, F_{exch} and U_{exch} , respectively, at ambient temperature under nondenaturing conditions in aqueous buffer.⁶ The interconversion between folded and unfolded states of the drkN SH3 domain is slow on the NMR chemical shift time scale⁷ ($<0.5 \text{ s}^{-1}$ at 5°C), thereby giving rise to two distinct sets of resonances corresponding to the F_{exch} and U_{exch} states, facilitating measurement of pK_a values for the unfolded ensemble.

Results and Discussion

Figure 1 illustrates the pulse scheme that was developed for measuring ^{13}C carboxyl chemical shift values of Asp and Glu residues in unfolded proteins. The magnetization transfer

* To whom correspondence should be addressed. E-mail: kay@bloch.med.utoronto.ca.

[†] Hospital for Sick Children.

[‡] Department of Biochemistry, University of Toronto.

[§] Departments of Medical Genetics and Chemistry, University of Toronto.

^{||} Protein Engineering Network Centers of Excellence.

- (1) Joshi, M. D.; Sidhu, G.; Pot, I.; Brayer, G. D.; Withers, S. G.; McIntosh, L. P. *J. Mol. Biol.* **2000**, *299*, 255–79.
- (2) Joshi, M. D.; Sidhu, G.; Nielsen, J. E.; Brayer, G. D.; Withers, S. G.; McIntosh, L. P. *Biochemistry* **2001**, *40*, 10115–39.
- (3) Anderson, D. E.; Becktel, W. J.; Dahlquist, F. W. *Biochemistry* **1990**, *29*, 2403–8.
- (4) Wang, Y. X.; Freedberg, D. I.; Yamazaki, T.; Wingfield, P. T.; Stahl, S. J.; Kaufman, J. D.; Kiso, Y.; Torchia, D. A. *Biochemistry* **1996**, *35*, 9945–50.

- (5) Schaefer, M.; Sommer, M.; Karplus, M. *J. Phys. Chem. B* **1997**, *101*, 1663–1683.

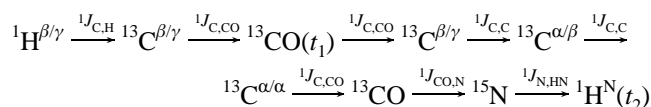
- (6) Zhang, O.; Forman-Kay, J. D. *Biochemistry* **1995**, *34*, 6784–6794.

- (7) Farrow, N. A.; Zhang, O.; Forman-Kay, J. D.; Kay, L. E. *Biochemistry* **1995**, *34*, 868–878.



Figure 1. Pulse scheme used to correlate ^{13}CO chemical shifts of Glu/Asp side-chain carboxyl groups with the backbone amide proton chemical shift of the following residue. All narrow (wide) bars correspond to rf pulses with a flip angle of 90° (180°), applied with phase x unless indicated otherwise. ^1H and ^{15}N carriers are centered at the water frequency and 119 ppm, respectively, and pulses applied with field strengths of 37 (^1H) and 6.4 (^{15}N) kHz, with the exception of the water selective 90° flip-back²⁴ pulses used in the WATERGATE²⁵ solvent suppression scheme (rectangular pulses with a field strength of 0.16 kHz). A 1.0 kHz WALTZ-16 decoupling field²⁶ is applied on nitrogen during acquisition. The ^{13}C carrier is initially set to 39.1 ppm (the center of $\text{C}^\beta(\text{Asp})/\text{C}^\gamma(\text{Glu})$ chemical shift regions in the drkN SH3 domain U_{exch} state), jumped to 179.6 ppm prior to the ^{13}CO pulse of phase ϕ_1 , jumped back to 39.1 ppm after gradient g_6 , and then jumped to 179.6 ppm after gradient g_{10} . All $^{13}\text{C}^{\text{aliph}}$ pulses prior to point e , with the exceptions of the shaped pulses, A , B and C , are applied as rectangular 90° (180°) pulses with a field strength of $\Delta/\sqrt{15}$ ($\Delta/\sqrt{3}$), where Δ is the separation in Hertz between the centers of the $^{13}\text{C}^{\text{aliph}}$ (39.1 ppm) and ^{13}CO (179.6 ppm) chemical shift regions.²⁷ The shaped pulses A and B have RE-BURP profiles²⁸ (2.5 ms, centered at 41.1 ppm and 442 μs , centered at 39.1 ppm, respectively; 500 MHz), while pulse C is an I-BURP-2 inversion pulse²⁸ (2.75 ms, 43.0 ppm). Note that pulse A refocuses the chemical shift of $\text{C}^\beta(\text{Asp})/\text{C}^\gamma(\text{Glu})$ carbons without excitation of $\text{C}^\alpha(\text{Asp})$ or $\text{C}^\beta(\text{Glu})$ spins, while pulse C inverts $\text{C}^\beta(\text{Asp})$ magnetization without affecting $\text{C}^\beta(\text{Glu})$ or $\text{C}^\alpha(\text{Asp})/\text{C}^\alpha(\text{Glu})$ spins. The final $^{13}\text{C}^{\text{aliph}}$ 180° pulse (rectangular, centered at 55 ppm) is applied with a field strength of $\Delta'/\sqrt{3}$, where Δ' is the separation between ^{13}CO and $^{13}\text{C}^\alpha$ spins. All ^{13}CO 90° pulses are rectangular with a field strength of $\Delta/\sqrt{15}$ (prior to e) or $\Delta'/\sqrt{15}$ (after e); ^{13}CO 180° pulses have a g_3 profile (335 μs)²⁹ until point e , while the final two ^{13}CO 180° pulses are rectangular with a field strength of $\Delta'/\sqrt{3}$. All off-resonance rectangular carbon pulses are generated by phase modulation of the carrier.^{30,31} Arrows indicate the positions of Bloch–Siegert compensation pulses.³² Values of the delays are $\tau_a = 1.8$ ms, $\tau_b = 4.5$ ms, $\tau_c = 7.0$ ms, $\eta = 4.5$ ms, $T_N = 12.5$ ms, $\delta_1 = 0.9$ ms, $\delta_2 = 5.5$ ms, $T = 2.6$ ms. The delays τ_x and τ_y are given by $\tau_x = \tau_c - \tau_b$ and $\tau_y = \tau_b - 1/2\tau_c$, respectively. The phase cycling employed is $\phi_1 = \{x, -x\}$, $\phi_2 = 4\{x\}$, $4\{-x\}$, $\phi_3 = 8\{x\}$, $8\{-x\}$, $\phi_4 = 2\{x\}$, $2\{-x\}$, and $\phi_{\text{rec}} = \{x, -x, -x, x\}$. Quadrature detection in F_1 is achieved via States-TPPI³³ of ϕ_1 . Gradient strengths in G/cm (durations in ms) are $g_1 = 8$ (0.5), $g_2 = 8$ (0.3), $g_3 = 20$ (1.0), $g_4 = 5$ (0.5), $g_5 = 7$ (0.8), $g_6 = 12$ (0.5), $g_7 = 8$ (0.4), $g_8 = 10$ (0.5), $g_9 = 8$ (0.5), $g_{10} = 6$ (1.0), $g_{11} = 10$ (0.5), $g_{12} = 14$ (0.8), $g_{13} = 5$ (0.6).

pathway can be summarized succinctly according to:



where the one-bond scalar couplings responsible for the transfer are indicated above the arrows, and t_1 , t_2 denote periods during which chemical shift is recorded. To optimize the sensitivity of the experiment, we have exploited the narrow chemical shift ranges for aliphatic carbon spins in unfolded protein states⁸ (see below). Magnetization originating on $\text{H}^\beta(\text{Asp})/\text{H}^\gamma(\text{Glu})$ is transferred to the $\text{C}^\beta(\text{Asp})/\text{C}^\gamma(\text{Glu})$ aliphatic carbon spins and then further on to the side-chain carboxyl $\text{C}^\gamma(\text{Asp})/\text{C}^\delta(\text{Glu})$ spins via the homonuclear one-bond $\text{C}^{\text{aliph}}\text{—CO}$ scalar coupling. The selective carbon 180° pulse A refocuses both $\text{C}^\beta(\text{Asp})$ (40.8–41.6 ppm in drkN SH3, U_{exch} state) and $\text{C}^\gamma(\text{Glu})$ (35.8–36.1 ppm) chemical shifts without affecting $\text{C}^\alpha(\text{Asp})$ (53.7–55.1 ppm) or $\text{C}^\beta(\text{Glu})$ (29.5–30.3 ppm) spins, so that magnetization can be transferred to the side-chain carboxyl carbon optimally (point a). Subsequently, transverse CO magnetization evolves during t_1 . Between points b and c , magnetization evolves under the influence of one-bond $\text{C}^{\text{aliph}}\text{—CO}$ (~ 55 Hz) and $\text{C}^{\text{aliph}}\text{—C}^{\text{aliph}}$ couplings (~ 35 Hz) for durations of $2\tau_b \approx 1/(2^1J_{\text{C,CO}})$ and $2\tau_c \approx 1/(2^1J_{\text{C,C}})$, respectively, and at point c the signal is transferred to $\text{C}^\alpha(\text{Asp})$ and $\text{C}^\beta(\text{Glu})$. By the end of the following transfer step ($2\tau_c$), after point d , transverse C^α in-phase (Asp) and anti-

phase (Glu, anti-phase with respect to C^β) magnetization has been established. Subsequently, transverse anti-phase magnetization with respect to the backbone CO is generated (the one-bond $\text{C}^{\text{aliph}}\text{—CO}$ coupling is active for a time $2\tau_b$ during the interval extending from points d to e), while the anti-phase magnetization of $\text{C}^\alpha(\text{Glu})$ with respect to C^β is refocused during $2\tau_c$. During this interval, in-phase magnetization of $\text{C}^\alpha(\text{Asp})$ is maintained by the application of two selective carbon 180° pulses, C , which invert $\text{C}^\beta(\text{Asp})$, but do not excite either $\text{C}^\alpha(\text{Asp})$ or $\text{C}^\alpha(\text{Glu})/\text{C}^\beta(\text{Glu})$. Finally, magnetization is transferred to the H^{N} amide spin of the subsequent residue via successive steps involving the large one-bond $^{13}\text{CO}\text{—}^{15}\text{N}$ and $^1\text{H}^{\text{N}}\text{—}^{15}\text{N}$ couplings.

Fourier transformation of the resulting 2-D data set gives peaks centered at $[\omega_{\text{CO}}(i), \omega_{\text{H}^{\text{N}}}(i + 1)]$, as shown in Figure 2 (inserts). Cross-peaks can be assigned on the basis of backbone amide proton chemical shifts obtained in $^1\text{H}\text{—}^{15}\text{N}$ HSQC correlation experiments. Ambiguities arising from overlapping $^1\text{H}^{\text{N}}$ shifts at a particular pH are often resolved by following $^1\text{H}^{\text{N}}$ chemical shift changes in the course of the pH titration. With regard to overlap in unfolded proteins, it should be noted that the present experiment is far superior to existing schemes which correlate side-chain CO and aliphatic proton chemical shifts. For example, in the U_{exch} state of the drkN SH3 domain (pH 6, 5 $^\circ\text{C}$), $^1\text{H}^{\text{N}}$ chemical shifts of residues following Asp and Glu cover a range of 0.50 ppm (8.19–8.69 ppm), while the dispersion for H^β (Asp, 2.56–2.75 ppm) and H^γ (Glu, 2.25–2.32 ppm) chemical shift values is much less. The pulse scheme can be readily extended to a sensitivity-enhanced three-

(8) Wishart, D. S.; Bigam, C. G.; Holm, A.; Hodges, R. S.; Sykes, B. D. *J. Biomol. NMR* **1995**, *5*, 67–81.

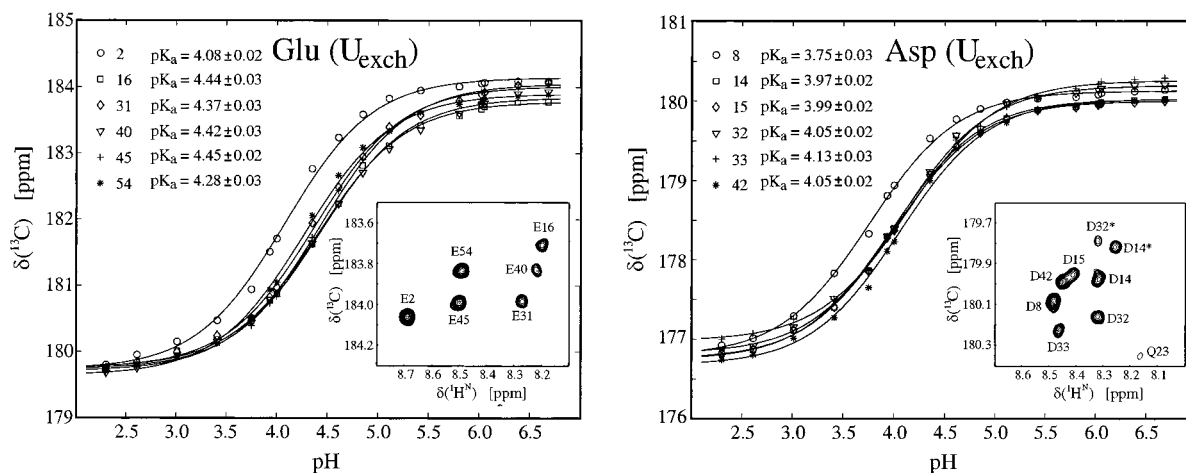


Figure 2. Experimental titration curves obtained for the unfolded state of the drkN SH3 domain. The pH profiles of chemical shifts were fitted to the Henderson–Hasselbach equation,²² with best fit pK_a values for each residue given in the upper left corner. Inserts show representative side-chain carboxyl $^{13}\text{CO}/\text{backbone amide } ^{15}\text{N}$ correlation maps of the drkN SH3 domain at 5 °C and pH 6.0 recorded at 500 MHz using the pulse scheme of Figure 1. All cross-peaks are labeled by residue number, and peaks arising from the F_{exch} state are indicated with an asterisk.

dimensional experiment by recording ^{15}N chemical shifts, producing a data set with correlations at $[\omega_{\text{CO}}(i), \omega_{\text{N}}(i + 1), \omega_{\text{H}}(i + 1)]$, thereby taking advantage of the favorable dispersion of ^{15}N chemical shifts in unfolded states.^{9,10}

As described above, the present experiment has been designed for unfolded proteins by exploiting the narrow chemical shift range for side-chain $\text{C}^\beta(\text{Asp})/\text{C}^\gamma(\text{Glu})$ carbon resonances. The increased dispersion of chemical shifts in folded protein states can make selective refocusing of $\text{C}^\gamma(\text{Glu})$ (i.e., without excitation of $\text{C}^\beta(\text{Glu})$, pulse A) difficult. For example, a 2.5 ms pulse centered at 41.1 ppm refocuses magnetization between 34.9 and 47.3 ppm, leaving spins upfield (downfield) of 30.5 ppm (51.7 ppm) unaffected (500 MHz). In the F_{exch} state of the drkN SH3 domain, the $\text{C}^\gamma(\text{Glu})$ shifts range from 35.0 to 36.4 ppm, while C^β shifts are surprisingly downfield, even for a folded protein, and vary between 30.7 and 33.7 ppm. It is, therefore, not possible to refocus $\text{C}^\gamma(\text{Glu})$ without affecting $\text{C}^\beta(\text{Glu})$, leading to sensitivity decreases. However, by application of a nonselective 180° pulse (A) and concomitant shortening of the delay τ_b (to ~ 3.2 ms) prior to point a, the experiment can be used to obtain correlations in both folded and unfolded proteins. In this case, however, cross-peaks from the unfolded state are attenuated by approximately 30%. Using this modification, we were able to measure pK_a values for residues in the folded state; a correlation between pK_a values in the U_{exch} and F_{exch} states and protein stability for the wild-type protein and a number of mutants will be forthcoming.

pK_a values of carboxyl groups in denatured states of a number of proteins have been estimated to be on average 0.3–0.4 pH units lower than those of model compounds (e.g., the peptides AlaAspAla and AlaGluAla with N- and C-terminal blocking groups),¹¹ likely due to local and/or nonlocal electrostatic interactions within a compact unfolded state ensemble.^{12–15}

Recently, computational techniques based on finite-difference Poisson–Boltzmann methods^{5,16} or on continuum electrostatics treatments¹⁷ have been employed to predict side-chain carboxyl pK_a values of Asp and Glu residues of unfolded proteins, also suggesting general average downward shifts (by 0.2–0.4 pH units) relative to model compounds. Our experimental data on the U_{exch} state of the drkN SH3 domain do not, however, indicate such a general trend, as shown in Figure 2. Notable deviations from model compound pK_a values (4.0 for Asp and 4.4 for Glu)¹¹ are measured for only two residues in the U_{exch} ensemble. Asp8 displays a downward shifted pK_a value of 3.75, which can most likely be attributed to a local electrostatic interaction with the side chain of His7. The pK_a of Glu2 is also shifted to a lower than average value (4.08), probably due to a local interaction with the positively charged N-terminus of the protein. The average pK_a values of all other Asp and Glu residues in the U_{exch} state (4.04 ± 0.06 and 4.39 ± 0.07 , respectively) compare well with model compound pK_a values. (Of interest, pK_a values in the F_{exch} state range from 4.0 to 4.6 for Glu and from 2.2 to 4.3 for Asp). The results for the U_{exch} state suggest that although the local sequence does have an effect on pK_a values, a general trend toward lower than model compound pK_a values is not found for the unfolded state ensemble of the drkN SH3 domain. The lack of long-range electrostatic interactions is likely due to the fact that the Asp and Glu side chains are all localized to the surface of the protein in the folded state and, thus, in any nativelike compact state conformation within the unfolded state ensemble.¹⁸

In summary, we have presented a pulse scheme optimized for measuring pK_a values of Asp and Glu side-chain carboxylates in unfolded protein states and applied this methodology to obtain, for the first time, residue-specific pK_a values for an unfolded protein. Data sets of relatively high sensitivity have been obtained on samples with concentrations as low as approximately 0.3 mM in unfolded protein in relatively modest acquisition times (~ 2 h), facilitating measurement of complete titration profiles. It is anticipated that the pulse scheme will be a valuable addition to the family of NMR experiments that has

(9) Zhang, O.; Forman-Kay, J. D.; Shortle, D.; Kay, L. E. *J. Biomol. NMR* **1997**, *9*, 181–200.

(10) Dyson, H. J.; Wright, P. E. *Nat. Struct. Biol.* **1998**, *5*, 499–503.

(11) Nozaki, Y.; Tanford, C. *J. Biol. Chem.* **1967**, *242*, 4731–4735.

(12) Tan, Y.-J.; Oliveberg, M.; Davis, B.; Fersht, A. R. *J. Mol. Biol.* **1995**, *254*, 980–992.

(13) Oliveberg, M.; Arcus, V. L.; Fersht, A. R. *Biochemistry* **1995**, *34*, 9424–9433.

(14) Swint-Kruse, L.; Robertson, A. D. *Biochemistry* **1995**, *34*, 4724–4732.

(15) Whitten, S. T.; Garcia-Moreno, E. B. *Biochemistry* **2000**, *39*, 14292–14304.

(16) Warwicker, J. *Protein Sci.* **1999**, *8*, 418–425.

(17) Elcock, A. H. *J. Mol. Biol.* **1999**, *294*, 1051–1062.

(18) Choy, W. Y.; Forman-Kay, J. D. *J. Mol. Biol.* **2001**, *308*, 1011–32.

currently been developed to characterize the structure and dynamics of unfolded protein states.

Materials and Methods

A uniformly ¹⁵N, ¹³C labeled sample of the N-terminal SH3 domain from the protein drk was prepared as described previously.⁹ Spectra were recorded on a 0.6 mM sample (total protein concentration, F_{exch} + U_{exch}), 50 mM sodium phosphate, 92% H₂O/8% D₂O. All spectra were recorded with widths of 1200 (8000) Hz with 128 (512) complex points in the indirect (direct) dimensions, corresponding to acquisition times of 107 (64) ms. Sixteen scans were recorded per FID, giving rise to a net acquisition time of 1.6 h/spectrum. Linear prediction was applied to the ¹³C dimension,¹⁹ and both dimensions were apodized with shifted squared sine-bell window functions, zero-filled, and Fourier transformed using the NMRPipe/NMRDraw suite of programs.²⁰ Chemical shifts were referenced relative to an internal standard DSS.²¹ Although F_{exch} and U_{exch} states are present in an ~1:1 ratio (at pH 6), cross-peaks from the F_{exch} state are typically of lower intensity than cross-peaks from the U_{exch} state since the experiment has been optimized for studies of unfolded states. pH profiles of chemical shifts were fit to the Henderson–Hasselbach equation,²²

$$\delta_{\text{exp}} = \frac{\delta_A + \delta_B 10^{(\text{pH}-\text{p}K_a)}}{1 + 10^{(\text{pH}-\text{p}K_a)}} \quad (1)$$

where δ_A and δ_B are the plateau values of carboxyl carbon chemical shifts in the acidic and basic pH limits, respectively.

- (19) Zhu, G.; Bax, A. *J. Magn. Reson.* **1992**, *98*, 192–199.
 (20) Delaglio, F.; Grzesiek, S.; Vuister, G. W.; Zhu, G.; Pfeifer, J.; Bax, A. *J. Biomol. NMR* **1995**, *6*, 277–293.
 (21) Wishart, D. S.; Bigam, C. G.; Yao, J.; Abildgaard, F.; Dyson, H. J.; Oldfield, E.; Markley, J. L.; Sykes, B. D. *J. Biomol. NMR* **1995**, *6*, 135–40.
 (22) Shrager, R. E.; Cohen, J. S.; Heller, S. R.; Sachs, D. H.; Schechter, A. N. *Biochemistry* **1972**, *11*, 541–547.

The pH of each sample was measured in the NMR tube before and after acquisition of each spectrum. To estimate the errors in pK_a values due to uncertainties in measured pH values, a Monte Carlo fitting procedure was employed²³ in which pH values are obtained from a normal distribution around the average pH meter reading with a standard deviation (estimated from repeat readings) of 0.05 pH units. The 250 profiles so obtained are subsequently fit with eq 1 to produce a distribution of pK_a values. Errors on the order of ±0.02 are obtained.

Acknowledgment. We thank Dr. D. R. Muhandiram (University of Toronto) for assistance with NMR experiments and Karin Crowhurst (Hospital for Sick Children, Toronto) for providing the sample. The research was supported by grants from the Canadian Institutes of Health Research (J.D.F.-K. and L.E.K.). M. T. is a recipient of an E. Schrodinger Fellowship (J-2086) of the Austrian Science Fund.

Supporting Information Available: One pulse scheme of a 3-D enhanced sensitivity experiment for measuring pK_a values in unfolded protein states which records ¹⁵N chemical shifts (PDF). This material is available free of charge via the Internet at <http://pubs.acs.org>.

JA020066P

- (23) Kamith, U.; Shriver, J. W. *J. Biol. Chem.* **1989**, *264*, 5586–5592.
 (24) Grzesiek, S.; Bax, A. *J. Am. Chem. Soc.* **1993**, *115*, 12593–12594.
 (25) Piotto, M.; Saudek, V.; Sklenar, V. *J. Biomol. NMR* **1992**, *2*, 661–5.
 (26) Shaka, A. J.; Keeler, J.; Frenkiel, T.; Freeman, R. *J. Magn. Reson.* **1983**, *52*, 335–338.
 (27) Kay, L. E.; Ikura, M.; Tschudin, R.; Bax, A. *J. Magn. Reson.* **1990**, *89*, 496–514.
 (28) Geen, H.; Freeman, R. *J. Magn. Reson.* **1991**, *93*, 93–141.
 (29) Emsley, L.; Bodenhausen, G. *Chem. Phys. Lett.* **1987**, *165*, 469–476.
 (30) Boyd, J.; Soffe, N. *J. Magn. Reson.* **1989**, *85*, 406–413.
 (31) Patt, S. L. *J. Magn. Reson.* **1992**, *96*, 94–102.
 (32) Vuister, G. W.; Bax, A. *J. Magn. Reson.* **1992**, *98*, 428–435.
 (33) Marion, D.; Ikura, M.; Tschudin, R.; Bax, A. *J. Magn. Reson.* **1989**, *85*, 393–399.